Atmospheric Electricity Studies at the Pierre Auger Observatory

Signal Comparisons between Lightning and Cosmic Ray Events

Kevin-Druis Merenda[1,*] on behalf of the Pierre Auger Collaboration[2,**,***]

[1]Colorado School of Mines, Golden, CO, USA
[2]Av. San Martín Norte 304, 5613, Malargüe, Argentina

Abstract. The research horizons of the Pierre Auger Cosmic-Ray Observatory widened when the collaboration found exotic (atmospheric) phenomena in both its Fluorescence Detector (FD) and Surface Detector (SD). The Cosmology and Geophysics task force of the Auger Collaboration focused some of its attention on these highly energetic events, which are correlated to some of the most intense convective thunderstorm systems in the world. In this proceeding, we compare the signal of these exotic events and the signal of cosmic rays, as seen in the FD and the SD. The FD has triggered on numerous transient luminous events, dubbed “elves" since their first observation in 2005. The SD observed peculiar events with radially expanding footprints, which are correlated with lightning strikes reconstructed by the World Wide Lightning Location Network (WWLLN). The traced signals of both of these atmospheric events last longer in time than cosmic ray signals. The footprints are much larger; typically more SD stations (or more FD pixels) contribute to the observations.

1 Introduction

1.1 The Pierre Auger Observatory

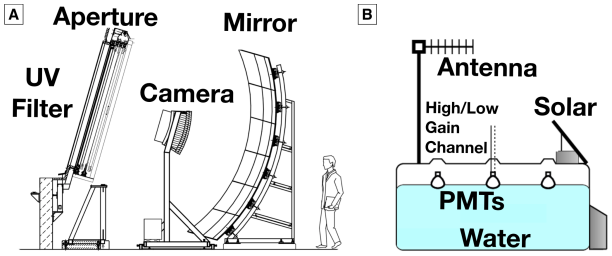

Figure 1. Panel A: one Schmidt telescope of the Auger FD. The light enters on the left through an aperture with a 2.2 m diameter. The aperture window has a UV filter to select the UV photons of the nitrogen fluorescence. The mirror has a 3.6 m diameter. The camera has 440 pixels, each with a 100 ns time resolution. Panel B: An SD station of area 10 m^2 and depth 1200 mm, filled with purified water, has three PMTs with a 25 ns resolution. Ultra-relativistic charged particles traveling through the detector create Cherenkov light recorded by the PMTs.

The primary focus of the Auger Observatory is to record the air showers produced by cosmic rays and reconstruct the direction, energy, and type of the primary particles [1]. To detect these air showers, the observatory uses a hybrid design consisting of a Surface Detector (SD) [2] and a Fluorescence Detector (FD) [3]. Most of the physics associated with an extensive air-shower of the highest energies can be done from the data of these two detectors.

The Auger FD has 24 telescopes distributed among four different sites; each site has an azimuthal field of view (FoV) of 180°. Each telescope has a $30° \times 30°$ FoV and an entrance aperture extended to 2.2 m diameter by a corrector ring. The light enters the telescope through a UV filter, to then be reflected by a 3.6 m diameter mirror onto the camera, which contains 440 photomultiplier tubes (Figure 1, panel A). The PMTs are hexagonally shaped, each with a FoV of 1.5°, and the camera consists of 22 rows and 20 columns. The time resolution of the FD is 100 ns. Due to the operational limitations of the FD, dark nights and clear weather, the duty cycle is 14%.

The SD is a 3000 km^2 array of ≈1600 water-Cherenkov stations. The stations have 1.5 km spacing and are placed in a triangular grid. For the reconstruction of cosmic rays, we search for an elementary cell made from a hexagonal crown with six stations at the corners and one station in the center. As shown in Figure 1, panel B, each tank has three photomultiplier tubes with a high-gain and a low-gain channel. The time resolution of each station is 25 ns. The duty cycle of the SD is almost 100%, making it the statistical engine of the observatory at the highest energies of the cosmic-ray spectrum.

Both detectors have three levels of triggering algorithms. Besides prescaled second level trigger (SLT) readouts, every event is required to pass a third level trigger (TLT). By searching the unanalyzed data of the prescaled SLTs, collaborators have found events consistent with lightning related physics: 1) elves in the FD and 2) anomalous events in the SD. The elve events are Emissions of Light from Very low frequency perturbations due to Elec-

*e-mail: kmerenda@mines.edu
**e-mail: auger_spokespersons@fnal.gov
***Authors list: http://www.auger.org/archive/authors_2018_10.html

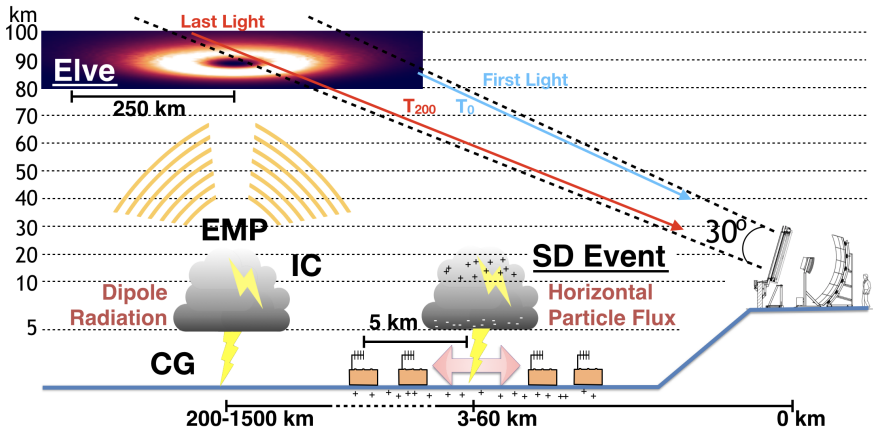

Figure 2. The FD sites are located on small hills above the SD. Due to atmospheric properties, cloud heights do not reach above 20 km. Negative cloud-to-ground lightning discharges are a few kilometers long. Two different phenomena are demonstrated in this diagram. Left: the return stroke process creates an electromagnetic pulse (EMP) which radiates to the ionosphere at 90 km altitude. When the EMP reaches the plasma, it creates a radially expanding flash of light, referred to as an 'elve'. The light at the nearest edge of the disk reaches the FD first, while the light above the lightning strike arrives later. Right: the cloud electrification induces positive charges on the ground. When the charges from the cloud travel downward to the ground, they will meet with the positive charges traveling upward to the cloud. This phenomenon is referred to as the attachment process. The attachment point of two, very localized leader tips, each with mega-volts of electric potential, may possibly be the source of particles seen in the SD.

tromagnetic pulse Sources [4] and the anomalous events are particle fluxes related to lightning. Since these discoveries, TLT algorithms specific to those events have been designed and optimized to improve the acquisition of events related to atmospheric electricity.

1.2 Atmospheric Electricity Physics at the Pierre Auger Observatory

The Auger Observatory is located in one of the most active regions on Earth for the creation of severe and convective thunderstorm systems [5]. The Cordoba and Mendoza provinces of Argentina, close to the Andes mountain range, are regularly exposed to destructive weather phenomena such as hail, tornadoes, floods, and lightning. Weather forecast simulations have shown that global warming will lead to an increased number of such storms across the globe [6]. Researching these extreme phenomena today will provide us with a glimpse of what is to come. This region is also believed to have the highest lightning flash rate per minute in the world for the most extreme lightning events [7]. Some of the instruments designed for cosmic-ray detection at the Auger Observatory are state-of-the-art detectors for lightning-related phenomena. We believe the lightning-related process which produces the anomalous SD observations is different from the process which creates the elves observed in the FD.

A lightning strike can be broken down into sequential steps [8]: the initial breakdown, the step leader propagation, the attachment process, the return stroke, the continuing current, the dart leader propagation, and the subsequent return strokes. Due to the convective motion of ice crystals, thunderstorms will form a few charge layers separated by kilometers in altitude. The electrified cloud will induce a charge onto the ground. Lightning discharges will generally happen between layers (intra-cloud , IC) or between the cloud and the ground (cloud-to-ground, CG). The first five steps mentioned above are all active research areas, with some processes understood better than others. A quasi-static electric field is constantly present due to the charge distribution of the cloud, which may contribute to the acceleration process of particles seen in the SD. The propagation of the leader takes tens of milliseconds. Most of the charges are placed in the tip of the step leader, localizing mega-volt potentials in a very small region. Then, the downward-propagating step leader meets the upward-propagating positive charges, close to the ground, at the attachment point. This step of the lightning process is not understood, and it has been hypothesized that the few microseconds preceding it are responsible for terrestrial gamma ray flashes. It is not unreasonable to consider the presence of a strong potential difference between the two leader tips, which could act as an initial acceleration mechanism for the particles detected in the SD. A few microseconds after the attachment, the return stroke process begins. The negative charges remaining in the channel flow towards the ground to neutralize with the positive charges flowing from the ground. In less than 10 microseconds, the current reaches its maximum. This fast time variation of the current creates a strong Electromagnetic Pulse (EMP). The EMP is the underlying process behind the elve events observed in the FD. Return strokes with a few hundred kilo-amperes have already been recorded by ground-based lightning detection networks. The subsequent return strokes have a much lower peak current, and occur every few milliseconds. Hence, elves from these strokes are either too dim for us to see or outside our acquisition time.

The FD has been observing lightning-related events over the Cordoba region, despite 650 km separating both locations (see Figure 2). The sharp current variation in the lightning return stroke, which is the brightest phenom-

ena in the lightning process, creates a very low frequency EMP which propagates to the ionosphere. At first contact with the ionosphere, right above the lightning strike, the energy density is enough to accelerate charged particles in the ionospheric plasma. The electrons will collide non-elastically with the local molecules and excite them. The actuated nitrogen fluorescence process will radiate photons in the form of a radially expanding ring that may reach radii beyond 250 km. The intensity of this emission is so bright that the FD can record such rings up to 1500 km away. Typical cosmic-ray events are only seen as far as 30 km. During the 2014-2016 period, we recorded an average of 500 elves per year.

When thunderstorms are over the array, the FD is turned off, but the SD still records information. We observed anomalous SD events with at least one station with a signal dominated by high-frequency noise. It could be due to the propagation of the lightning EMP, similar in frequency to radio waves, through the wires. Moreover, these events are characterized by stations with a signal which lasts more than 10 μs, about two orders of magnitude more than the duration of a signal produced by a cosmic muon. For these stations, we looked at the ratio between the high-gain and low-gain channels, expecting a value equal to the amplification factor between the two channels. We know what the amplification factor should be if the signal is really produced by particles that cross the water in the station. Additionally, we checked also that the three PMTs of the station collected the same signal profile. Finally, we searched for a correlation between our events and lightning strikes detected by the World Wide Lightning Location Network (WWLLN) [9].

2 Observation of Elves in the Fluorescence Detector

The Auger Collaboration has reported on elves numerous times in other proceedings [10] and a journal paper is about to be published on a subset of the data. However, a convenient side-by-side comparison of a cosmic-ray signal and an elve has not yet been emphasized.

In panels A and B of Figure 3, we display the signal of a typical elve with only one peak in the photo-trace. The time of the peak maximum is shown on the color axis in panel A. The expansion of the elve is projected onto the camera. It lasts longer than the current FD acquisition time of 300 microseconds. The signal propagates across the camera and away from the pixel that first triggered. The first light that reaches the detector originates from a point on the ionosphere halfway between the lightning strike and the camera. That halfway point is the shortest distance for light to travel from the lightning strike, to the ionosphere and then to the FD camera. Hence, photons arriving after the first light reveal the light from an elve which is mostly fully expanded. As the acquisition time gets longer, the emission pattern above the lightning strike reveals the hole from the dipole radiation pattern. The radius of that hole is correlated to the speed of the electrons in the channel, during the return stroke process [11]. UV fluorescence is

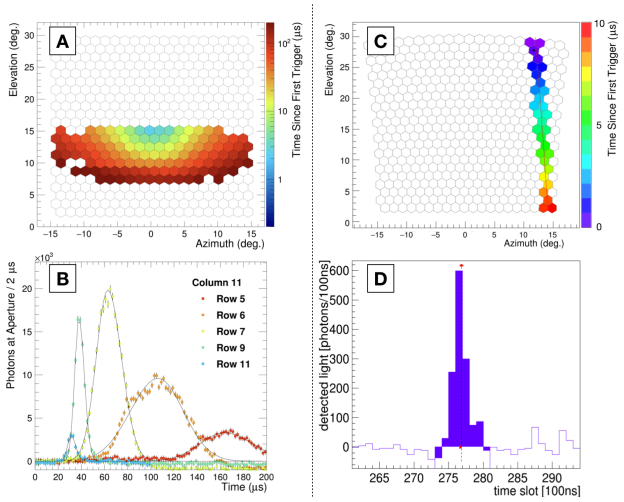

Figure 3. The comparison between the elve signal (panels A and B in the left column) and the cosmic-ray signal (panels C and D in the right column) in the FD. The distinctions to focus on are the amplitude and length of the traces, as well as the signal geometry on the camera. Panel A: a time projection of the elve onto the camera. The time of the peak maximum was chosen for the log color scale. Each hexagon is a FD pixel. Panel B: Selected pixel traces of column 11. All traces were binned every two microseconds to limit the clutter on the plot and fitted with a skewed Gaussian distribution. Panel C: a time projection of a cosmic ray onto the camera. The black dot, in the purple pixel, shows the selected trace presented in panel D. Panel D: One selected trace of a pixel high in the camera, with the location of the fitted peak maximum.

a process which lasts approximately 40 ns [12], which is a lot shorter than the intrinsic time width of the EMP (10 microseconds). Hence, recording the UV emission of the elve is equivalent to the direct observation of the propagating EMP. The fitted traces of selected pixels are shown in panel B of Figure 3. As the edge of the elve is dimmer than the regions close to the center, the amplitude of the traces in the upper rows of the camera is small compared to the maximum light observed. The geometric projection of the dipole radiation onto to the ionosphere, at 92 km, causes the maximum brightness of an elve to occur between 50 and 100 km from its center. When projected to the base of the ionosphere, pixels at the bottom of the camera view a larger surface area of the ionosphere than the ones in the upper rows. This distortion causes lower elevation pixels to integrate light from more ionosphere than higher elevation pixels. Hence, the traces become wider and more asymmetric when looking along a column, as we show in panel B of Figure 3. Some lightning strikes may create multiple EMPs, resulting in multi-peaked traces in the FD. Traces are well fitted with a skewed Gaussian, the basis for the current reconstruction of the event. From elve events confirmed with a visual scan, we are able to reconstruct the geodetic location and current profile of the lightning strike.

In contrasts with panels A and B, the time propagation of a cosmic-ray shower is presented in panel C, and a selected trace is shown in panel D. The selected trace is

the one of the pixel marked with a black dot in panel C of Figure 3. As the extended air-shower propagates close to the speed of light, a typical cosmic-ray signal lasts about 500 nanoseconds in each pixel. The total shower development across the FoV of the telescope is less than 10 microseconds. The number of photons seen by the FD is indicative of the energy of the electromagnetic component of the shower, which is related to the total energy of the primary particle. Typically, showers are not seen beyond 30 km from the individual FD sites unless their energy is very high. The local arrival direction of the cosmic ray plays a significant role in the distribution of light across the camera.

3 Observation of Anomalous Events in the Surface Detector

The critical details of the underlying phenomena responsible for the anomalous events observed in the SD are still a mystery. We have done our event selection based on how the signal observed in the SD stations differs from a typical cosmic-ray signal [13]. When reconstructing a cosmic-ray shower in the SD, the footprint is required to be at least bigger than the crown described in introduction (Figure 4, panel D). The black line represents the reconstructed arrival direction of the cosmic ray projected onto the ground. The color portrays the time, with purple for earlier signal and red for later signal. The footprint of a typical cosmic-ray shower is less than 5 km. In panel E, we displayed the trace observed in one of the PMTs of an SD station, showing a sharp signal that lasts about one microsecond.

The anomalous events have a very distinct signal that expands radially from a central source. The signal closest to the center is the largest. The amplitude of the signal across the stations decreases as a function of distance from the center. By using the start time of each signal pulse and performing a spherical fit, the location of the source was consistently reconstructed to be very close to the ground. Two different anomalous events are shown in panels A and B of Figure 4, and the typical traces of one SD station are shown in panel C. For 2004 to 2017, a preliminary scan found more than 100 events which did not match a typical footprint of a cosmic-ray shower. A verification scan was performed on this set to select 28 events with long traces in the stations. Most of the events happened in 2007 and 2008, with rarer occurrences in later years. We found that 70% of the larger events that passed strict cuts necessary for a good reconstruction are correlated with lightning strikes observed by WWLLN. In the field of view of the observatory, WWLLN is believed to be 70% efficient for lightning strikes of the highest energies.

So far, the footprints of the large anomalous events were ring shaped. The average size of the rings was about 6 km. In recent studies, we have found that the ring shape may be due to a cosmic-ray trigger algorithm not optimized for the acquisition of these lightning-related events. Hence we now expect that these peculiar events are actually disks.

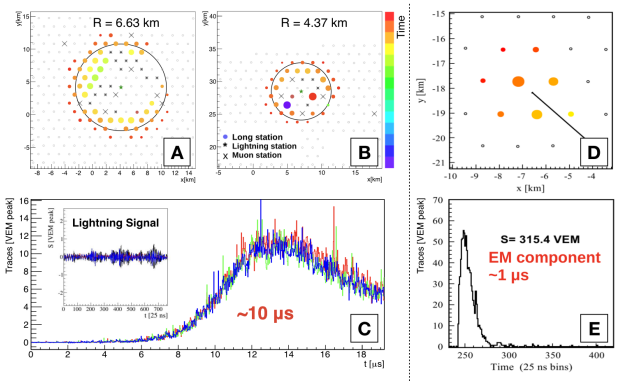

Figure 4. The comparison between the signal of the anomalous events (panels A, B and C in the left column) and the signal of cosmic-ray showers (panels D and E in the right column) in the SD. The large footprint and the longer traces of the atmospheric events are the distinguishable features. Panels A and B: two different events recorded by the SD, which are known to be correlated with lightning. Each dot represents an SD station, with the time of the peak shown as the color and the intensity portrayed by the size of individual disks. A simple circular fit is performed to estimate the size of the event. The reader should note the additional presence of stations triggered by lightning. Panel C: example traces of the three PMTs in a station that represent the signal of an anomalous event. The smaller plot is there to provide a contrast of those traces with lightning-triggered stations. Panel D: the typical footprint of a cosmic-ray shower detected towards the center of the SD. The meaning behind the size and color of the marker is the same as for the anomalous events. The black line represents the reconstructed arrival direction of the cosmic ray, projected onto the ground. Panel E: a typical trace in an SD station for a cosmic-ray event, dominated by time propagation of the electromagnetic component of the shower.

4 Future Work

We do not know if the anomalous SD events are correlated to previously observed lightning phenomena, making the research very exploratory. We performed the reconstruction of these events and we defined several characteristics which can help us find their interpretation. An extensive study of prescaled SLT data is necessary to define a dedicated trigger and acquire more statistics. This additional statistics (and looser cuts) will help us understand the phenomenon we are observing.

On the other hand, the underlying process of elves is well understood by the geophysics community, but we are trying to assess if the quality of the data is sufficient to enable groundbreaking studies of new regimes of lightning physics. Do the existing lightning models describe the most extreme energy lightning strikes correctly? A spatio-temporal reconstruction of elves already exists. We want to know how much energy is needed to create them, and we will use our large statistics to provide distributions of the fundamental parameters necessary to create the EMP: peak current, current rise time, return stroke speed, channel length, and ionosphere height.

5 Acknowledgments

The authors wish to thank the World Wide Lightning Location Network (wwlln.net), a collaboration among over 50 universities and institutions, for providing the lightning location data used in this paper.

References

[1] A. Aab, P. Abreu, M. Aglietta et al., Nuclear Instruments and Methods in Physics Research Section A: Accelerators, Spectrometers, Detectors and Associated Equipment **798**, 172 (2015)

[2] I. Allekotte, A. Barbosa, P. Bauleo et al., Nuclear Instruments and Methods in Physics Research Section A: Accelerators, Spectrometers, Detectors and Associated Equipment **586**, 409 (2008)

[3] J. Abraham, P. Abreu, M. Aglietta et al., Nuclear Instruments and Methods in Physics Research Section A: Accelerators, Spectrometers, Detectors and Associated Equipment **620**, 227 (2010)

[4] H. Fukunishi, Y. Takahashi, M. Kubota, K. Sakanoi, U.S. Inan, W.A. Lyons, Geophysical Research Letters **23**, 2157 (1996)

[5] K.L. Rasmussen, M.D. Zuluaga, R.A. Houze, Geophysical Research Letters **41**, 7359 (2014)

[6] J.T. Seeley, D.M. Romps, J.T. Seeley, D.M. Romps, Journal of Climate **28**, 2443 (2015)

[7] E.J. Zipser, D.J. Cecil, C. Liu, S.W. Nesbitt, D.P. Yorty, Bulletin of the American Meteorological Society **87**, 1057 (2006)

[8] V. Rakov, M. Uman, IEEE Transactions on Electromagnetic Compatibility **40**, 403 (1998)

[9] M.L. Hutchins, R.H. Holzworth, J.B. Brundell, C.J. Rodger, Radio Science **47**, 1 (2012)

[10] R. Mussa, G. Ciaccio, The European Physical Journal Plus **127**, 94 (2012)

[11] P.R. Blaes, R.A. Marshall, U.S. Inan, Geophysical Research Letters **41**, 9182 (2014)

[12] F. Valk, M. Aints, P. Paris, T. Plank, J. Maksimov, A. Tamm, Journal of Physics D: Applied Physics **43**, 385202 (2010)

[13] R. Colalillo, Proceedings of Science **ICRC2017** (2017)